J Nanopart Res (2009) 11:77–89
DOI 10.1007/s11051-008-9446-4

Characterization of size, surface charge, and agglomeration state of nanoparticle dispersions for toxicological studies

Jingkun Jiang · Günter Oberdörster · Pratim Biswas

Received: 25 May 2008 / Accepted: 4 June 2008 / Published online: 25 June 2008

Abstract Characterizing the state of nanoparticles (such as size, surface charge, and degree of agglomeration) in aqueous suspensions and understanding the parameters that affect this state are imperative for toxicity investigations. In this study, the role of important factors such as solution ionic strength, pH, and particle surface chemistry that control nanoparticle dispersion was examined. The size and zeta potential of four TiO_2 and three quantum dot samples dispersed in different solutions (including one physiological medium) were characterized. For 15 nm TiO_2 dispersions, the increase of ionic strength from 0.001 M to 0.1 M led to a 50-fold increase in the hydrodynamic diameter, and the variation of pH resulted in significant change of particle surface charge and the hydrodynamic size. It was shown that both adsorbing multiply charged ions (e.g., pyrophosphate ions) onto the TiO_2 nanoparticle surface and coating quantum dot nanocrystals with polymers (e.g., polyethylene glycol) suppressed agglomeration and stabilized the dispersions. DLVO theory was used to qualitatively understand nanoparticle dispersion stability. A methodology using different ultrasonication techniques (bath and probe) was developed to distinguish agglomerates from aggregates (strong bonds), and to estimate the extent of particle agglomeration. Probe ultrasonication performed better than bath ultrasonication in dispersing TiO_2 agglomerates when the stabilizing agent sodium pyrophosphate was used. Commercially available Degussa P25 and in-house synthesized TiO_2 nanoparticles were used to demonstrate identification of aggregated and agglomerated samples.

Keywords Nanoparticle · Toxicology · Nanotoxicology · Health · Safety · Ultrasonication · Nanotechnology · Environment

J. Jiang · P. Biswas (✉)
Aerosol and Air Quality Research Laboratory, Department of Energy, Environmental and Chemical Engineering, Washington University in St. Louis, St. Louis, MO 63130, USA
e-mail: pratim.biswas@wustl.edu

G. Oberdörster
Department of Environmental Medicine, University of Rochester, Rochester, NY 14642, USA

Introduction

Engineered nanoparticles (<100 nm) are synthesized to achieve unique physicochemical properties and functionalities, and are finding applicability in many commercial products. However, these unique properties that make nanomaterials valuable for numerous applications also have the potential to increase their adverse impacts (The Royal Society 2004). Findings from epidemiological, clinical, and animal studies with ultrafine particles that are in the same size range as engineered nanoparticles indicate that exposure to

these particles can cause significant adverse health effects (Oberdorster et al. 1994; U.S. EPA 2004; von Klot et al. 2005). Recently toxicological studies with certain engineered nanoparticles have confirmed that nanoparticles can be potentially harmful due to their high specific surface area and unique physicochemical properties (Oberdorster 2004; Hoshino et al. 2004; Magrez et al. 2006). The term nanotoxicology has been coined that aims to establish the relationship between nanoparticle physicochemical properties (e.g., size, surface properties, and crystal phase) and their toxic potential (Oberdorster et al. 2005a, b, 2007; Jiang et al. 2008).

To correlate properties of the nanoparticles to their toxicity potential and ensure that results are reproducible and meaningful, accurate characterization of nanoparticles at different stages such as synthesized or as supplied, as administrated, and after administration is essential (Oberdorster et al. 2005a; Powers et al. 2006; Jiang et al. 2008). Until the relationships between nanoparticle characteristics and toxicity are fully understood, it will be necessary to ensure that all nanomaterial characteristics that are potentially significant are measured or can be derived in toxicity screening tests. However, the determination of every possible characteristic of a nanomaterial is impractical. An important set of properties has been identified that must be addressed in toxicological studies, and include size, state of dispersion, surface charge, shape, chemical composition, surface area, and surface chemistry- (Oberdorster et al. 2005a, b; Powers et al. 2006). Synthesis methods have been developed to produce nanoparticles with very well-defined and tightly controlled characteristics. The properties can also be evaluated after synthesizing or receiving test nanoparticles in powder form (Jiang et al. 2007, 2008). However, characterization of nanoparticles in the actual biological test (as administered and after administering) is essential since potential physicochemical changes (e.g., agglomeration state and surface charge variation) can occur while in solution. These changes may have a significant impact on observed toxicological responses (Powers et al. 2007).

The hydrodynamic size and surface charge of nanoparticle dispersions can have a dramatic effect on the way in which an organism responds upon exposure, and these need to be properly characterized. The size of nanoparticle governs its interactions with biological systems, including absorption, distribution, metabolism, and excretion (Renwick et al. 2001; Borm et al. 2006; Choi et al. 2007). Surface characteristics affect agglomeration in dispersions and the nanoparticle hydrodynamic size distributions can be altered by a small change of particle surface charge. The uptake and translocation of nanoparticles by organisms are also affected by their surface charge (Hoshino et al. 2004). For example, nanoparticle surface charge has been observed to alter blood-brain barrier integrity and permeability (Lockman et al. 2004). The characterization of these two properties has been proposed in several nanotoxicology review articles (Oberdorster et al. 2005a; Powers et al. 2006, 2007); however, there are very few studies that have systematically examined them. Murdock et al. (2008) characterized the hydrodynamic size and surface charge of different nanoparticles (such as Ag, TiO_2, and carbon nanotubes) in biologically relevant solutions. While observational results are reported in their study, the important factors that control the state of nanoparticle dispersion, such as solution ionic strength (IS), pH, surface charge, and surface coating, are not discussed.

Knowledge of the controlling parameters of dispersion state will have significant implications on sample preparation for toxicological studies and biological response interpretation. It has been shown that using unstable and agglomerated nanoparticle dispersions in an in vitro or in vivo experiment could lead to inaccurate assessment of nanoparticle toxicity and even misleading conclusions (Warheit et al. 2004; Shvedova et al. 2005). Several studies have investigated the influences of different dispersing media in preparing stable nanoparticle dispersions (Buford et al. 2007; Sager et al. 2007). It was found that when nanoparticles are dispersed in liquids, their hydrodynamic size is often larger than the primary particle size. Understanding the stability and agglomeration behavior of nanoparticles under different solution conditions will facilitate these investigations. Even if the hydrodynamic sizes of nanoparticles suspended in physiological media are determined to be larger than their primary sizes, it is important to know whether these particles are in an agglomerated (weak bonds between primary particles) or aggregated (hard bonds between primary particles) state, since their corresponding biological fate and effects will be different. The stability of nanoparticle

dispersions and their tendency to agglomerate can be considered in the context of electrostatic, steric, and van der Waals forces between particles using the Derjaguin-Landau-Verwey-Overbeek (DLVO) theory (Derjaguin and Landau 1941; Verwey and Overbeek 1948).

In this study, the size and zeta potential of seven nanoparticle samples dispersed in different solutions were characterized. The effects of ionic strength and pH on the state of dispersion are studied using titanium dioxide nanoparticles as a model. The criteria to prepare stable dispersions, including electrostatic and steric stabilization, are examined using dispersions of TiO_2 nanoparticles and quantum dots with different surface groups. The influence of different ultrasonication methodologies on the resultant hydrodynamic size of particles is discussed. Methodologies to determine nanoparticle agglomeration/aggregation state are investigated.

Materials and methods

The alteration of characteristics of dry nanoparticle powders when added to a liquid is illustrated in Fig. 1. Nanoparticles in the dry state can be in two forms: aggregated (hard bonds between primary particles due to sintering) and agglomerated (held by weaker van der Waals forces). The state of nanoparticles, either aggregated or agglomerated, can be controlled during synthesis (Jiang et al. 2007; Tsantilis and Pratsinis 2004). After dispersing nanoparticles in solution, they can remain as singlets or form agglomerates, or remain as aggregates, surrounded by an electrical double layer (Fig. 1). Typically, when agglomerated nanoparticle samples are added to a liquid they can be separated by overcoming the weaker attractive forces by several methodologies, whereas the aggregated nanoparticles cannot be separated. Depending on the objective of a toxicological study, a certain state of the

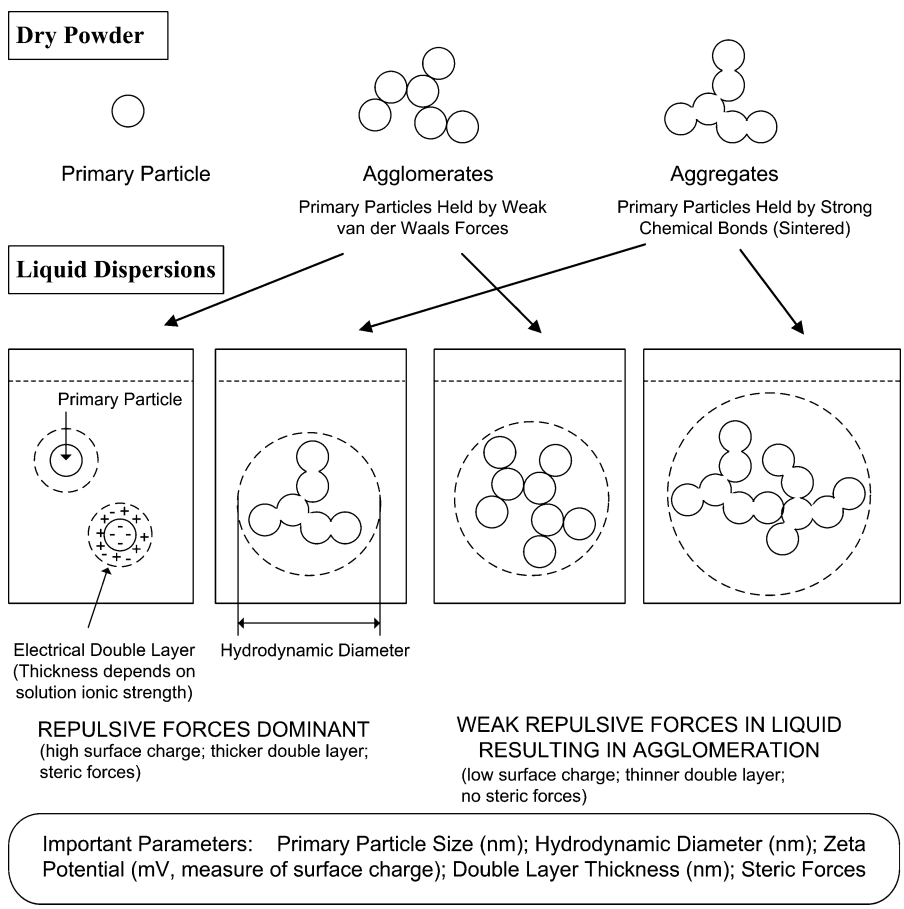

Fig. 1 Various states and configurations of particles in dry state and when dispersed in liquids

particles that can represent realistic exposure scenarios should be selected. For instance, nanoparticles retained as singlets would be preferential to establish the biological responses as a function of primary particle size. It should also be noted that only the final equilibrium state of the suspension is characterized in this work, and any kinetic mechanisms or pathways to the final structures are beyond the scope of the present study.

Chemicals

Seven different nanoparticles were used in this study, as listed in Table 1. Anatase TiO_2 (H) and (S) with primary particle sizes of 15 nm and 26 nm, respectively, and specific surface areas of 102.1 m^2/g and 61.5 m^2/g, respectively, were synthesized via a flame aerosol reactor (Jiang et al. 2007, 2008). The precursor used to synthesize TiO_2 particles was titanium tetra-isopropoxide (Sigma Aldrich, St. Louis, Missouri), and was fed into the reactor by a bubbler. TiO_2 (P25) with a primary particle size of 27 nm, a specific surface area of 57.4 m^2/g, and a phase composition of 80% anatase and 20% rutile was purchased from Degussa Chemicals (Hanau, Germany). Anatase TiO_2 (F) with a primary particle size of 195 nm and a specific surface area of 8.0 m^2/g was purchased from Fisher Scientific (Fairlawn, New Jersey). Quantum dots (QDs) with three different surface groups were purchased from Invitrogen (Eugene, Oregon). These QDs are core-shell cadmium selenide-zinc sulfide nanocrystals coated with polyethylene glycol (PEG), amine-terminated polyethylene glycol (PEG–NH_2), and carboxylic-terminated polyethylene glycol (PEG–COOH), respectively. The primary size of uncoated nanocrystalline QDs was reported to be approximately 2.3–5.5 nm (Dabbousi et al. 1997). Other chemicals used in this study include sodium chloride (NaCl), physiological saline (0.9% NaCl), sodium pyrophosphate ($Na_4P_2O_7$), sodium hydroxide (NaOH), and hydrogen chloride (HCl). Physiological saline (0.9% NaCl) was purchased from Hospira (Lake Forest, Illinois). All other chemicals were purchased from Sigma Aldrich (St. Louis, Missouri). All chemicals are pyrogen free.

Size and surface charge analysis

The hydrodynamic size and the surface charge (zeta potential) of nanoparticle dispersions were characterized with a ZetaSizer Nano ZS (Malvern Instruments Inc, UK) utilizing dynamic light scattering (DLS) and

Table 1 Summaries of experiments performed

Case	Nanoparticles	Solvents	Objective
1	TiO_2 (H)[a]	DI H_2O; 0.001–0.1 M NaCl	Determine the ionic strength effect on dispersion characteristics
2	TiO_2 (H)	Solutions with the same ionic strength 0.001 M and different pH (3.4–10.4) by adding HCl, NaCl, or NaOH	Determine the pH effect on dispersion characteristics
3	TiO_2 (H)	DI H_2O; 0.0001–0.01 M $Na_4P_2O_7$; 0.005 M $Na_4P_2O_7$ + NaCl (0.005–0.05 M)	Study dispersion electrostatic stabilization
4	Quantum dots[b] (PEG), (PEG–NH_2), (PEG–COOH)[b]	Physiological saline (0.15 M/0.9% NaCl)	Study dispersion steric stabilization
5	TiO_2 (H), (P25)[c], (F)[d], (S)[e]	DI H_2O; 0.005 M $Na_4P_2O_7$	Test the effect of different sonication methodologies in preparing dispersions and identify whether sample is an agglomerate or aggregate

[a] 15 nm TiO_2 nanoparticles synthesized via a flame aerosol reactor (Jiang et al. 2008, 2007)

[b] Quantum dots (2.3–5.5 nm) purchased from Invitrogen

[c] 25 nm TiO_2 purchased from Degussa Chemicals

[d] 195 nm TiO_2 purchased from Fisher Scientific

[e] 26 nm TiO_2 nanoparticles synthesized via a flame aerosol reactor

electrophoretic light scattering (ELS), respectively. DLS is also known as photon correlation spectroscopy (PCS) and quasi-elastic light scattering (QELS). Particles in solution undergo Brownian motion due to random collisions between the solvent molecules and the particles. As a consequence of this particle motion, light scattering from the particle ensemble fluctuates with time. In DLS, the autocorrelation of these temporal fluctuations in scattered light intensity is evaluated to determine the intensity weighted average diffusion coefficient (m^2/s), D, of the particles. The average hydrodynamic diameter, d_p, can then be calculated from the diffusion coefficient using the Stokes–Einstein equation: $d_p = kT/3\pi\mu D$, where k is the Boltzmann constant ($J\ K^{-1}$), T is the absolute temperature (K), and μ is the viscosity of the medium ($kg\ m^{-1}\ s^{-1}$). The hydrodynamic diameter is the diameter of a sphere that has the same diffusion coefficient as the particles (Fig. 1). A single exponential decay is assumed when determining the average hydrodynamic diameter. Considering that multiple particle size groups are often present in the solution, a size distribution is necessary to describe the dispersion. By fitting the correlation curve to a multiple exponential form, the intensity size distribution can be determined. While DLS is the most well-developed and commonly used technique for hydrodynamic size distribution measurement, other light scattering-based techniques (Saltiel et al. 2004) and nanoelectrospray size spectrometry (Hogan et al. 2006; Lenggoro et al. 2007) can also be considered for the hydrodynamic diameter measurement.

ELS, also known as laser Doppler electrophoresis (LDE) or laser Doppler velocimetry (LDV), was used for zeta potential measurement. When an electric field is applied across the dispersion, charged particles in the dispersion will move toward the electrode of opposite polarity. This phenomenon is called electrophoresis. If a laser beam is passed through the sample undergoing electrophoresis, the scattered light from the moving particles will be frequency shifted. By measuring the frequency shift, the electrophoretic mobility ($m^2\ V^{-1}\ s^{-1}$), U, can be determined given the laser wavelength and the scattering angle. Zeta potential (V), ζ, can then be calculated from the electrophoretic mobility using the Smoluchowski equation: $\zeta = \mu U/\varepsilon$, where ε is the electric permittivity of the medium ($C^2\ N^{-1}\ m^{-2}$). It should be noted that in the surrounding electrical double layer there is a notional boundary (slipping plane), within which the liquid moves together with particles. The measured zeta potential is the potential at this slipping plane. It is not exactly the surface potential (surface charge), but is the potential of practical interest in dispersion stability because it determines the interparticle forces (Morrison and Ross 2002).

General experimental plan

The experimental plan is summarized in Table 1. Ionic strength (mol/L), IS, is a function of the concentration of all ions present in a solution: $IS = 0.5 \sum_{B=1}^{n} c_B z_B^2$, where c_B is the molar concentration of ion B (mol/L), and z_B is the charge number of ion B. To examine the IS effect on the hydrodynamic size and surface charge, 15 nm TiO_2 (H) nanoparticles were dispersed in NaCl solution with different molar concentrations (case 1). Since the addition of NaCl does not change the solution pH, TiO_2 dispersions with different ionic strength had the same pH value, $\sim$4.6. To determine the pH influence on the state of dispersion, TiO_2 (H) nanoparticles were dispersed in solutions with the same ionic strength (0.001 M) but different pH, which was adjusted by adding HCl, NaCl, NaOH, or a combination (case 2). The stability of dispersion is controlled by the interactions between particles. One can suppress particle coagulation (agglomeration) and increase the stability of nanoparticle dispersion by increasing interparticle repulsive forces: the electrostatic force (electrostatic stabilization) or the steric force (steric stabilization) (Kulkarni et al. 2003). In case 3, electrostatic stabilization was demonstrated by adding the dispersing agent sodium pyrophosphate in TiO_2 dispersions, which increased nanoparticle surface charge and the electrostatic repulsive force between particles. In case 4, steric stabilization was examined by dispersing polymer coated QDs in biologically relevant physiological saline solution (0.15 M/0.9% NaCl). The effect of ultrasonication methods (bath vs. probe sonication) on the state of the nanoparticle dispersions was examined in case 5. Different TiO_2 ((P25) and (S)) samples were used with these sonication methodologies to classify them as agglomerated or aggregated.

For most experiments, nanoparticles were dispersed in solutions at a concentration of approximately 50 μg/ml, and then sonicated for 5 min using a

bath sonicator (100 W, 42 kHz, Fisher Scientific, Fairlawn, New Jersey) before measuring the size and zeta potential. Longer sonication time using the bath sonicator did not change the dispersion size and surface charge. In case 5, probe sonicator (750 W, 20 kHz, Cole-Parmer, Vernon Hills, Illinois) was also used to disperse nanoparticles. As stated earlier, only the final equilibrium state of the suspension is characterized in this work. Typically, dilute solutions are used in toxicological studies, and tests were conducted to confirm the independence of the final hydrodynamic size and zeta potential for a range of mass concentrations (50–200 μg/ml). All results for the average size and the size distribution were averaged from more than five measurements, while those for the zeta potential were averaged from more than three measurements.

Results and discussion

The effects of ionic strength and pH on nanoparticle dispersion size and surface charge are presented first, followed by discussion of the electrostatic and steric stabilization of nanoparticle dispersions. Finally, the effect of different sonication methods in dispersing nanoparticles, and the use of those methods in distinguishing between agglomerates and aggregates are presented.

IS and pH effects

In DLVO theory (Derjaguin and Landau 1941; Verwey and Overbeek 1948), the agglomeration and stability of particle dispersions are determined by the sum of the attractive and repulsive forces between individual particles. The attraction between particles is due to the van der Waals force. The interaction of the electrical double layer surrounding each particle is called electrostatic repulsive force. When particles are coated by polymers, a steric repulsive force between particles needs to be included, though it is due to a rather entropy effect resulting from reducing polymer configurational freedom instead of a physical force (Ott and Finke 2007). The two important properties of the electrical double layer are the zeta potential and the thickness of the electrical double layer (Morrison and Ross 2002). An increase in either will result in an increase in the electrostatic repulsive interaction. The surface charge is controlled by several mechanisms, including surface ionization, ion adsorption, and lattice ion dissolution (Stumm and Morgan 1996), while the thickness of electrical double layer is a function of solution ionic strength, with an increase in IS leading to a decrease in double layer thickness. The DLVO approximation is not expected to hold at long separation distances for very low ionic strengths (Widegren and Bergstrom 2002). However, such conditions are rarely encountered in samples used in toxicological studies.

The average hydrodynamic diameter increases dramatically with increasing solution IS (Fig. 2). When TiO_2 (H) was dispersed in deionized water (IS $\approx 10^{-5}$ M) and 0.001 M NaCl, the average hydrodynamic diameters were similar ($\sim$90 nm) and the dispersions were stable, as the electrostatic repulsive force is dominant over the attractive force, suppressing agglomeration under such conditions. A modest increase in IS to 0.005 M resulted in a substantial size increase to approximately 156 nm. At a NaCl concentration of 0.1 M, the attractive force between particles became dominant over the repulsive force, resulting in an unstable, highly agglomerated dispersion. Under these conditions, the average

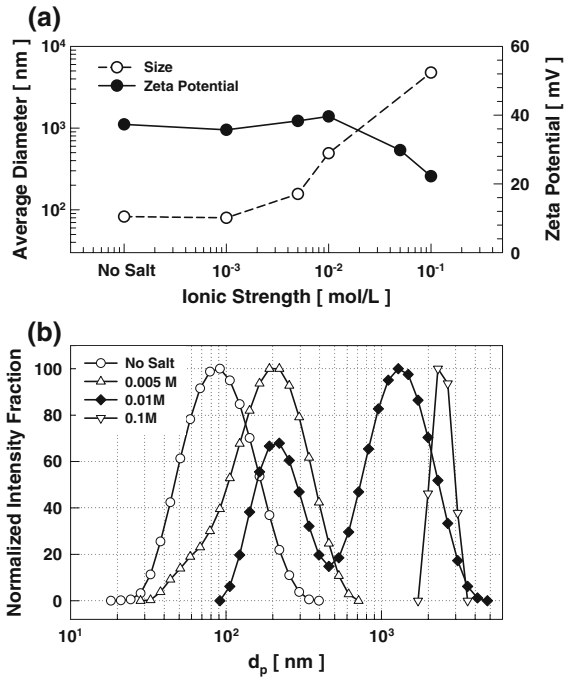

Fig. 2 The influence of the ionic strength on (**a**) the average hydrodynamic diameter and the zeta potential and (**b**) the size distributions of TiO_2 (H) dispersions

hydrodynamic size was 4780 nm, close to the upper limit of measurement of the instrument. DLVO interaction energy calculation for 15 nm TiO_2 nanoparticles gave similar results, i.e., the energy barrier to prevent agglomeration decreased with increasing solution ionic strength. In many toxicological studies, the IS of the buffer solution to disperse nanoparticles for in vitro and in vivo tests is often higher than 0.1 M (Long et al. 2006; Warheit et al. 2007; Sager et al. 2007; Murdock et al. 2008). Such conditions lead to unstable and highly agglomerated dispersions. The size distributions for selected dispersion conditions are shown in Fig. 2b. The trend is consistent with that for the average diameter, i.e., the size distributions shift toward larger size ranges with increasing ionic strength. Conversely, at low ionic strength there is no obvious change of dispersion zeta potential, while at an ionic strength above 0.01 M a substantial decrease in zeta potential with increasing ionic strength was observed (Fig. 2a). This is consistent with previous studies (Widegren and Bergstrom 2002; Brant et al. 2005) and predictions of the classical colloidal theory (Hunter 1981). As mentioned earlier, the zeta potential is the potential difference between the bulk and the slipping plane situated some distance from the particle surface (dependent on the electrical double layer thickness). Increasing ionic strength results in the compression of the electrical double layer. Hence, although the particle surface charge may be unchanged since sodium and chlorine ions do not interact with the TiO_2 particle surface, the zeta potential decreases with increasing ionic strength.

The dispersion surface charge (zeta potential) and consequently the hydrodynamic size can be altered by changing the solution pH. For mineral oxides and sulfides (e.g., TiO_2, SiO_2, and AsS) dispersed in water, surface ionization controls their surface charge in the absence of preferential adsorption of soluble ions in solution (Morrison and Ross 2002). At low pH such particles have a positive surface charge and, conversely, at high pH, a negative surface charge. The isoelectric point is the intermediate pH at with a particle has zero net surface charge. The zeta potential and average diameter of TiO_2 (H) dispersions as a function of pH with ionic strength held constant for all dispersions at 0.001 M are shown in Fig. 3. The measured isoelectric point for TiO_2 is approximately 6.0, which is consistent with isoelectric point measured elsewhere (Kosmulski 2002). Particles have a

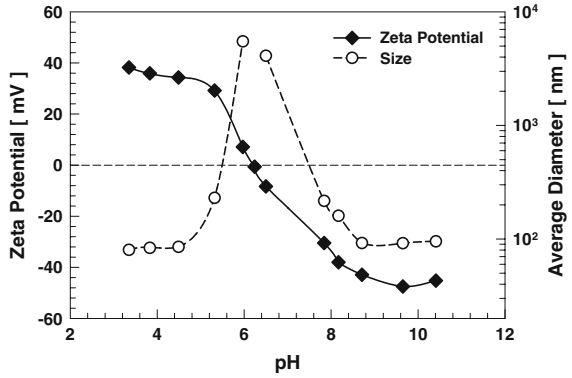

Fig. 3 The influence of solution pH on the zeta potential and the hydrodynamic diameter of TiO_2 (H) dispersions

positive zeta potential when pH is lower than 6, while the zeta potential is negative when pH is higher than 6. A strong correlation between the zeta potential and average size was observed (Fig. 3). When pH is far from the isoelectric point, the absolute value of zeta potential becomes higher. The electrostatic repulsive force is then dominant over the van der Waals force, such that agglomeration is suppressed. Consequently, the average size was small, ~90 nm, when pH was lower than 4.2 or higher than 8.2. When pH approaches the isoelectric point, the repulsive force is weakened due to low surface charge, and the hydrodynamic size increases beyond which it is measurable. Under these conditions, large flocs were formed which settled out of the solution due to gravitational forces in a short time.

Electrostatic and steric stabilization

The use of stable nanoparticle dispersions is often required to correlate nanoparticle physicochemical properties with their toxic potential. The general criterion to prepare stable dispersion is to increase repulsive forces between particles such that agglomeration is suppressed or is kinetically slow. As already demonstrated, electrostatic stabilization, i.e., adjustment of the pH to increase particle surface charge can increase the repulsive force between particles. However, in many toxicological tests, the pH has to be limited to a narrow range appropriate for healthy function of test cells and organisms. The surface charge can be alternatively controlled by use of a dispersing salt, which can dissociate into multiply charged ions. If a particle is ionic or has

highly polar bonds, multiply charged ions may be adsorbed by the particle in an aqueous environment, leading to an increase in particle surface charge and zeta potential. Examples of such salts are those containing polyphosphate, hexametaphosphate, pyrophosphate, and polysilicate anions.

The stabilization of TiO_2 nanoparticle dispersions using sodium pyrophosphate ($Na_4P_2O_7$) was examined. As shown in Fig. 4, the adsorption of pyrophosphate ions onto TiO_2 particle surfaces changed the zeta potential from positive (approximately 40 mV) to negative (approximately −53 mV). Though the ionic strength increases with increasing sodium pyrophosphate concentration, no change in the dispersion size distribution was observed up to the maximum $Na_4P_2O_7$ concentration tested (0.01 M). Furthermore, it should be noted that the IS of 0.01 M $Na_4P_2O_7$ is higher than that of 0.01 M NaCl. For comparison, another test was done by combining sodium pyrophosphate and sodium chloride. The concentration of sodium pyrophosphate was fixed at 0.005 M, while that of sodium chloride was increased from 0.005 M to 0.05 M. As shown in Fig. 5, no increase in the dispersion size was observed up to 0.01 M NaCl when $Na_4P_2O_7$ was used, compared to the dramatic increase over the same range of NaCl concentrations without $N_4P_2O_7$ (Fig. 2). With 0.05 M NaCl, a size increase was observed since the total IS was close to 0.1 M (Fig. 5). A rough criterion for electrostatic stabilization at low IS is that the absolute value of the zeta potential must be greater than 30 mV

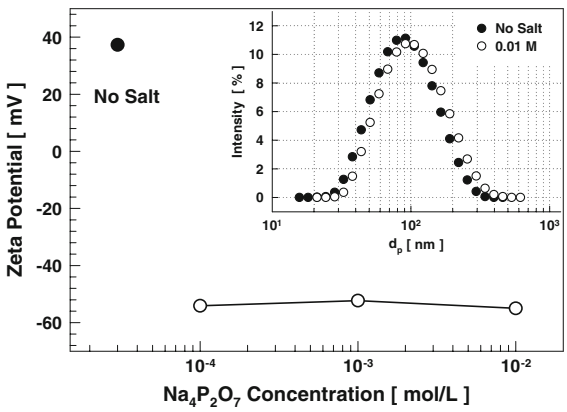

Fig. 4 The zeta potential of TiO_2 (H) dispersions as a function of sodium pyrophosphate ($Na_4P_2O_7$) concentration. Inset shows the particle size distributions of TiO_2 (H) in deionized water and in 0.01 M $Na_4P_2O_7$

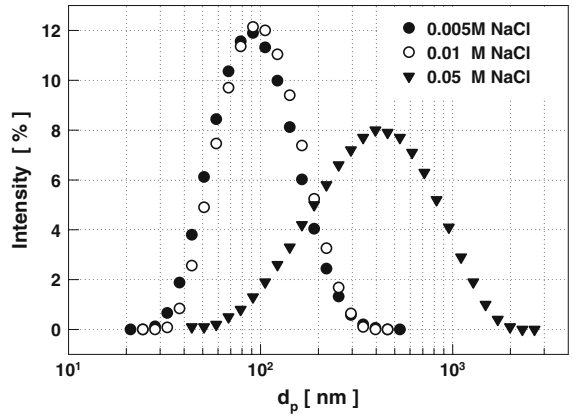

Fig. 5 The particle size distributions of TiO_2 (H) in mixtures of 0.005 M $Na_4P_2O_7$ and NaCl with three different concentrations

or that solution pH must be far from the isoelectric point by more than 2 if surface ionization is the dominant mechanism (ISO 14887 2000). As demonstrated here, either of these criteria can be met, and electrostatic stabilization can be used to prepare stable particle dispersions at low ionic strength.

Unfortunately, electrostatic stabilization is only efficient at low IS, less than ∼0.1 M. However, steric stabilization, achieved by coating nanoparticles with polymers, is possible at all solution IS. The size and zeta potential analysis of quantum dots with different surface coatings (PEG, PEG–NH_2, PEG–COOH) dispersed in physiological saline solution (0.15 M NaCl) is shown in Fig. 6. The polymer coating of QDs resulted in a steric repulsive force between particles. Therefore, stable dispersions were achieved even at high ionic strength (0.15 M). Intensity-based size distributions do bias toward large particles since one large particle can scatter several orders more light than one small particle. There are a few agglomerates of QDs which account for the larger peak in intensity-based size distributions. Since their quantity was low, the second peak disappears when plotting the volume-based distributions. Even in volume-based distributions, the average hydrodynamic diameter, 10–20 nm, is still higher than the primary particle diameter, 2.3–5.5 nm (Dabbousi et al. 1997). The primary particle diameter of QDs was determined by TEM, and is a number-based average. Just as there is a difference between intensity- and volume-based distributions, the volume-based hydrodynamic diameters also bias toward larger particles compared to

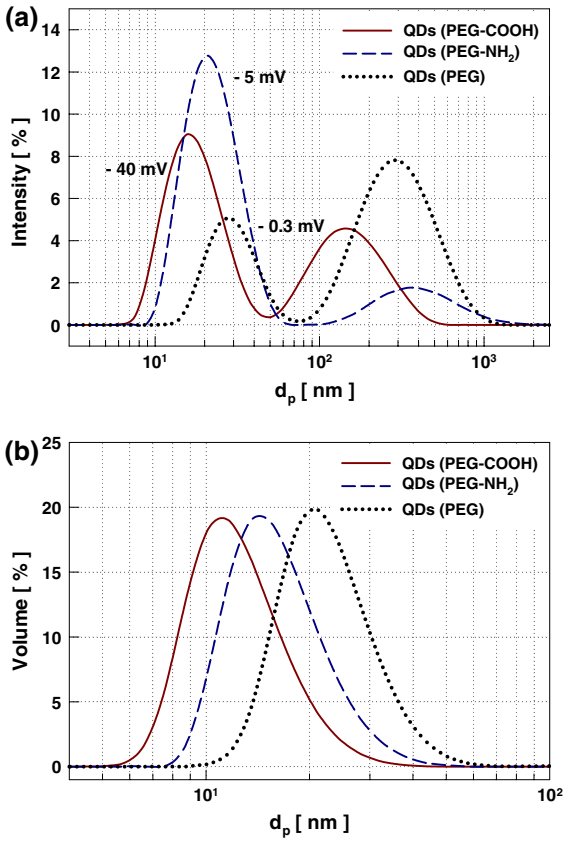

Fig. 6 (**a**) Intensity- and (**b**) volume-based particle size distributions for quantum dots (QDs) with different surface groups in physiological saline solution (0.15 M NaCl)

number-based average QD primary particle diameters. In addition, both the polymer coating and the surrounding electrical double layer on each nanocrystal add a certain thickness (Kim et al. 2004), and the interaction of long carbon chains may also contribute to the larger hydrodynamic size (Hoshino et al. 2004).

The difference of the size distributions of QDs with different surface groups was due to their different zeta potentials. In polymer-coated QD dispersions, electrostatic repulsive forces and steric repulsive forces exist simultaneously. The steric forces for three types of QDs are similar since they are all coated with polyethylene glycol. QDs with carboxylic-terminated polyethylene glycol surface modification had the highest surface charge (−40 mV) and their hydrodynamic size was the smallest, while QDs with PEG had the lowest surface charge (−0.3 mV) and the largest hydrodynamic size. It has been shown both theoretically and experimentally that the effectiveness of electrostatic stabilization increases with increasing particle size, whereas the effectiveness of steric stabilization increases with decreasing particle size (Morrison and Ross 2002). Therefore, the combination of electrostatic and steric stabilization, also referred to as electrosteric stabilization, by means of polymer coating containing one or more ionic charges (as demonstrated with carboxylic-terminated polyethylene glycol coatings on QDs) will allow for the stabilization of nanoparticle dispersions over a wide size range. Similar coating of nanoparticles by proteins and other compounds can occur during performance of in vivo toxicological studies, thus changing surface properties which will subsequently affect the stability of the dispersion (Wallace et al. 2007; Dutta et al. 2007; Brewer et al. 2005).

Dispersing nanoparticles and distinguishing agglomerates and aggregates

Many nanoparticle samples used in toxicological studies are received in powder form. Effectively dispersing them in solutions is often necessary for in vitro and in vivo tests. To disperse them, an external force to overcome the van der Waals attractions has to be applied. Ultrasonication is a commonly used technique to disperse agglomerates, as it can pull the liquid apart to form evacuated cavities or micro-voids. The formation and destruction of these cavities can impose a shear force on agglomerates, capable of overcoming the van der Waals force holding them together. However, the applied forces are not strong enough to break the hard bonds of aggregates. Simultaneously, cavity formation and destruction can also enhance agglomeration in the liquid by promoting interactions and contact of nanoparticles (kinematic coagulation). The effectiveness of dispersing nanoparticles is controlled predominantly by specific energy input, which is a function of dispersion volume, power, and time (Mandzy et al. 2005). Bath sonication and probe sonication are two commonly used ultrasonication methods. Bath sonication creates a pattern of active zones where cavitation takes place, and each of these has a low concentration of cavities, while probe sonication creates a single active zone with a high concentration of cavities.

Though TiO_2 (H) in deionized water formed a stable dispersion with a high zeta potential

(~40 mV), the hydrodynamic diameter (90 nm) was still much higher than the primary particle size (15 nm). About 5-min bath sonication was used to prepare the TiO_2 (H) dispersion. Longer sonication time was also tested, but did not change the particle size distribution. Conditions in the flame reactor were selected so as to obtain TiO_2 (H) nanoparticles that were not aggregated (Jiang et al. 2007). Similar methods were also used to prepare TiO_2 (P25) and (F) dispersions in deionized water. As shown in Fig. 7, the hydrodynamic diameters of TiO_2 (P25) and (F) dispersions in deionized water were significantly higher than the primary particle diameters of the powder samples, implying that bath sonication is not very effective in dispersing agglomerates.

Probe sonication was also tested for dispersing TiO_2 agglomerates. It was found that for TiO_2 (H) in deionized water, probe sonication can not only break agglomerates locally, but also promote agglomeration due to enhanced particle–particle interactions. Consequently, with increasing sonication time the dispersion hydrodynamic size decreased initially and then increased. This is consistent with the observations made by other researchers (Vasylkiv and Sakka 2001; Murdock et al. 2008). In contrast, no enhanced agglomeration was observed when bath sonication was used. To increase the surface charge and suppress the agglomeration, 0.005 M $Na_4P_2O_7$ was used to disperse the TiO_2 (H) nanoparticles. The dispersion was first bath sonicated for 5 min and then probe sonicated. The average diameter as a function of probe sonication time is shown in Fig. 8. After

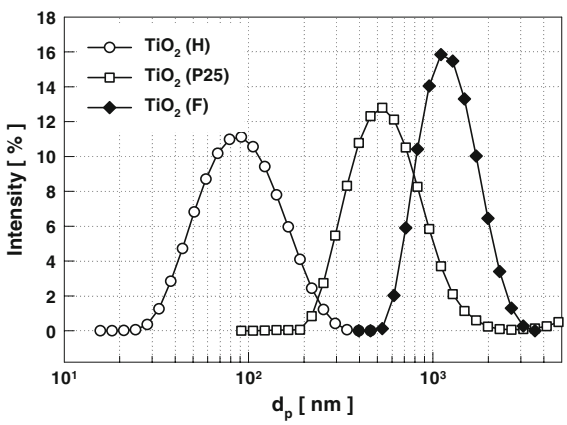

Fig. 7 Particle size distributions of TiO_2 (H), (P25), and (F) in deionized water

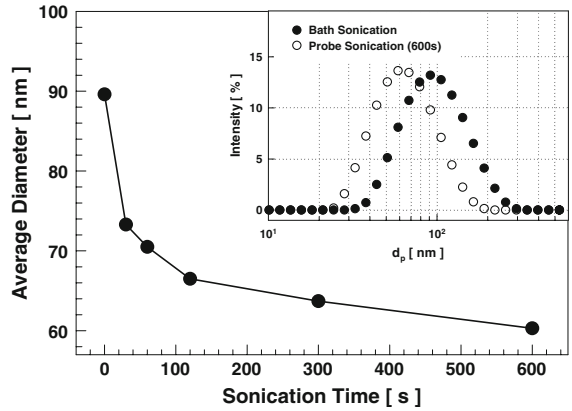

Fig. 8 The average hydrodynamic diameter of TiO_2 (H) in 0.005 M $Na_4P_2O_7$ as a function of probe sonication time. Inset shows particle size distributions of TiO_2 (H) in 0.005 M $Na_4P_2O_7$ after 5-min bath sonication and 10-min probe sonication

bath sonication, the hydrodynamic size was approximately 90 nm, consistent with previous tests. Sodium pyrophosphate was effective in preventing the further agglomeration via probe sonication by suppressing particle–particle growth due to enhanced electrostatic repulsive forces. The average hydrodynamic size decreased with increasing sonication time. After 10 min of probe sonication, the dispersion hydrodynamic diameter was comparable to the primary particle diameter. The possible explanations for the discrepancy have been discussed earlier. Under appropriately controlled conditions (addition of a salt), results here show that probe sonication is more effective than bath sonication in dispersing nanoparticle agglomerates.

The same method can be applied to determine the dispersion agglomeration/aggregation state. Degussa TiO_2 (P25) is commonly present as an aggregated sample with a primary particle size of ~27 nm. For comparison, an agglomerated TiO_2 (S) with similar primary particle size (~26 nm) was synthesized. Both TiO_2 (P25) and (S) in 0.005 M $Na_4P_2O_7$ were first bath sonicated for 5 min and then probe sonicated. After bath sonication the hydrodynamic diameter of agglomerated TiO_2 (S), ~140 nm, is only half of the aggregated TiO_2 (P25) hydrodynamic diameter, ~290 nm (Fig. 9). When probe sonication was applied, the hydrodynamic diameters of both dispersions decreased quickly within short sonication time and then became relatively constant with

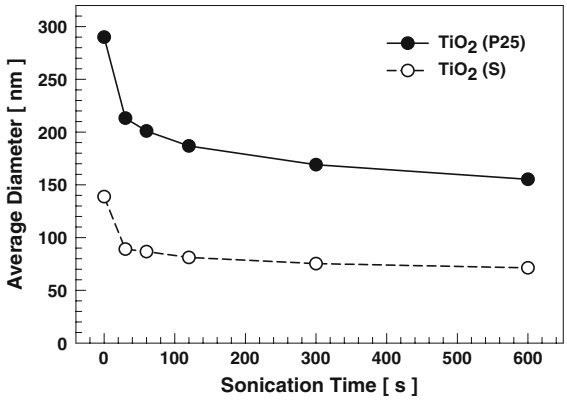

Fig. 9 The average hydrodynamic diameters of TiO_2 (P25) and (S) in 0.005 M $Na_4P_2O_7$ as a function of probe sonication time

increasing sonication time. After 10 min of probe sonication, the hydrodynamic diameter of TiO_2 (P25) dispersion ($\sim$155 nm) was distinctly larger than the primary particle size, which indicates that TiO_2 (P25) is composed largely of aggregates that cannot be readily broken up. This is consistent with previous observations (Mandzy et al. 2005; Teleki et al. 2008). Conversely, the hydrodynamic diameter of tailor-made TiO_2 (S) dispersion ($\sim$70 nm) was comparable to its primary particle size. Again, the possible explanations for the discrepancy have been discussed earlier. Knowing the smallest hydrodynamic diameter, one can estimate the relative agglomeration degree of nanoparticle dispersions at different conditions by comparing the hydrodynamic diameters. Other techniques such as mechanic milling (Muller et al. 2004) and high pressure system (Wengeler et al. 2006) are also useful to prepare singlet nanoparticle dispersions. For instance, it has been reported that when high pressure system was applied to TiO_2 (P25) dispersion, an additional small peak around 50 nm was observed due to sintering neck breakage (Teleki et al. 2008). However, the breakage of aggregates into singlets might not happen in the realistic exposure scenarios such that these techniques have limited application in toxicological studies.

Conclusions

Important parameters governing the state and stability of nanoparticle dispersions were examined and discussed in this study, including solution ionic strength, pH, surface charge, and surface coating. Ionic strength influences dispersion stability by changing the electrical double layer thickness, while pH can change the dispersion state by altering the zeta potential (surface charge). For instance, increasing ionic strength or bringing the pH close to the nanoparticle isoelectric point will enhance agglomeration and result in larger hydrodynamic sizes. Adsorbed multiply charged ions and polymer coatings on nanoparticle surfaces can suppress agglomeration and stabilize nanoparticle dispersions. Probe sonication and electrostatic stabilization work very well in dispersing nanoparticle agglomerates. The technique can also be used to determine if the sample contains aggregated particles which do not disperse in contrast to agglomerated samples. These results have important implications in performance of toxicological studies, such as preparation of nanoparticle dispersions for in vitro or in vivo tests and interpretation of biological responses. Similarly, additional dispersion characterization (size and surface charge) after nanoparticles are administrated in a test system or model will be particularly valuable to understand the relationship between nanoparticle properties and their toxicities, which is still limited by current technological capabilities of in situ measurement.

Acknowledgments This work was partially supported by a grant from the U.S. Department of Defense (AFOSR) MURI Grant, FA9550-04-1-0430. Support from the Center of Materials Innovation, Washington University in St. Louis, is also acknowledged.

References

Borm PJA, Robbins D, Haubold S, Kuhlbusch T, Fissan H, Donaldson K et al (2006) The potential risks of nanomaterial: a review carried out for ECETOC. Part Fibre Toxicol 3:11–46. doi:10.1186/1743-8977-3-11

Brant J, Lecoanet H, Wiesner MR (2005) Aggregation and deposition characteristics of fullerene nanoparticles in aqueous systems. J Nanopart Res 7:545–553. doi:10.1007/s11051-005-4884-8

Brewer SH, Glomm WR, Johnson MC, Knag MK, Franzen S (2005) Probing BSA binding to citrate-coated gold nanoparticles and surfaces. Langmuir 21:9303–9307. doi:10.1021/la050588t

Buford M, Hamilton R, Holian A (2007) A comparison of dispersing media for various engineered carbon nanoparticles. Part Fibre Toxicol 4:6. doi:10.1186/1743-8977-4-6

Choi HS, Liu W, Misra P, Tanaka E, Zimmer JP, Ipe BI et al (2007) Renal clearance of quantum dots. Nat Biotechnol 25:1165–1170. doi:10.1038/nbt1340

Dabbousi BO, RodriguezViejo J, Mikulec FV, Heine JR, Mattoussi H, Ober R et al (1997) (CdSe)ZnS core-shell quantum dots: synthesis and characterization of a size series of highly luminescent nanocrystallites. J Phys Chem B 101:9463–9475. doi:10.1021/jp971091y

Derjaguin BV, Landau LD (1941) Theory of the stability of strongly charged lyophobic sols and of the adhesion of strongly charged particles in solutions of electrolytes. Acta Physicochim URSS 14:733–762

Dutta D, Sundaram SK, Teeguarden JG, Riley BJ, Fifield LS, Jacobs JM et al (2007) Adsorbed proteins influence the biological activity and molecular targeting of nanomaterials. Toxicol Sci 100:303–315. doi:10.1093/toxsci/kfm217

Hogan CJ, Kettleson EM, Ramaswami B, Chen DR, Biswas P (2006) Charge reduced electrospray size spectrometry of mega- and gigadalton complexes: whole viruses and virus fragments. Anal Chem 78:844–852. doi:10.1021/ac051571i

Hoshino A, Fujioka K, Oku T, Suga M, Sasaki YF, Ohta T et al (2004) Physicochemical properties and cellular toxicity of nanocrystal quantum dots depend on their surface modification. Nano Lett 4:2163–2169. doi:10.1021/nl048715d

Hunter RJ (1981) Zeta potential in colloid science. Academic press Inc., London

ISO 14887 (2000) Sample preparation—dispersing procedures for powders in liquids

Jiang J, Chen DR, Biswas P (2007) Synthesis of nanoparticles in a flame aerosol reactor (FLAR) with independent and strict control of their size, crystal phase and morphology. Nanotechnology 18:285603. doi:10.1088/0957-4484/18/28/285603

Jiang J, Oberdorster G, Elder E, Gelein R, Mercer P, Biswas P (2008) Does nanoparticle activity depend upon size and crystal phase? Nanotoxicology 2:33–42. doi:10.1080/17435390701882478

Kim S, Lim YT, Soltesz EG, De Grand AM, Lee J, Nakayama A et al (2004) Near-infrared fluorescent type II quantum dots for sentinel lymph node mapping. Nat Biotechnol 22:93–97. doi:10.1038/nbt920

Kosmulski M (2002) The significance of the difference in the point of zero charge between rutile and anatase. Adv Colloid Interface 99:255–264. doi:10.1016/S0001-8686(02)00080-5

Kulkarni P, Sureshkumar R, Biswas P (2003) Multiscale simulation of irreversible deposition in presence of double layer interactions. J Colloid Interface Sci 260:36–48. doi:10.1016/S0021-9797(02)00236-9

Lenggoro IW, Widiyandari H, Hogan CJ, Biswas P, Okuyama K (2007) Colloidal nanoparticle analysis by nanoelectrospray size spectrometry with a heated flow. Anal Chim Acta 585:193–201. doi:10.1016/j.aca.2006.12.030

Lockman PR, Koziara JM, Mumper RJ, Allen DD (2004) Nanoparticle surface charges alter blood-brain barrier integrity and permeability. J Drug Target 12:635–641. doi:10.1080/10611860400015936

Long TC, Saleh N, Tilton RD, Lowry GV, Veronesi B (2006) Titanium dioxide (P25) produces reactive oxygen species in immortalized brain microglia (BV2): implications for nanoparticle neurotoxicity. Environ Sci Technol 40:4346–4352. doi:10.1021/es060589n

Magrez A, Kasas S, Salicio V, Pasquier N, Seo JW, Celio M et al (2006) Cellular toxicity of carbon-based nanomaterials. Nano Lett 6:1121–1125. doi:10.1021/nl060162e

Mandzy N, Grulke E, Druffel T (2005) Breakage of TiO2 agglomerates in electrostatically stabilized aqueous dispersions. Powder Technol 160:121–126. doi:10.1016/j.powtec.2005.08.020

Morrison ID, Ross S (2002) Colloidal dispersions: suspensions, emulsions, and foams. Wiley-Interscience, New York

Muller F, Peukert W, Polke R, Stenger F (2004) Dispersing nanoparticles in liquids. Int J Miner Process 74:S31–S41. doi:10.1016/j.minpro.2004.07.023

Murdock RC, Braydich-Stolle L, Schrand AM, Schlager JJ, Hussain SM (2008) Characterization of nanomaterial dispersion in solution prior to in vitro exposure using dynamic light scattering technique. Toxicol Sci 101:239–253. doi:10.1093/toxsci/kfm240

Oberdorster E (2004) Manufactured nanomaterials (Fullerenes, C-60) induce oxidative stress in the brain of juvenile largemouth bass. Environ Health Perspect 112:1058–1062

Oberdorster G, Ferin J, Lehnert BE (1994) Correlation between particle-size, in-vivo particle persistence, and lung injury. Environ Health Perspect 102:173–179. doi:10.2307/3432080

Oberdorster G, Maynard A, Donaldson K, Castranova V, Fitzpatrick J, Ausman K et al (2005a) Principles for characterizing the potential human health effects from exposure to nanomaterials: elements of a screening strategy. Part Fibre Toxicol 2:8. doi:10.1186/1743-8977-2-8

Oberdorster G, Oberdorster E, Oberdorster J (2005b) Nanotoxicology: an emerging discipline evolving from studies of ultrafine particles. Environ Health Perspect 113:823–839

Oberdorster G, Stone V, Donaldson K (2007) Toxicology of nanoparticles: a historical perspective. Nanotoxicology 1:2–25. doi:10.1080/17435390701314761

Ott LS, Finke RG (2007) Transition-metal nanocluster stabilization for catalysis: a critical review of ranking methods and putative stabilizers. Coord Chem Rev 251:1075–1100. doi:10.1016/j.ccr.2006.08.016

Powers KW, Brown SC, Krishna VB, Wasdo SC, Moudgil BM, Roberts SM (2006) Research strategies for safety evaluation of nanomaterials. Part VI. Characterization of nanoscale particles for toxicological evaluation. Toxicol Sci 90:296–303. doi:10.1093/toxsci/kfj099

Powers KW, Palazuelos M, Moudgil BM, Roberts SM (2007) Characterization of the size, shape, and state of dispersion of nanoparticles for toxicological studies. Nanotoxicology 1:42–51. doi:10.1080/17435390701314902

Renwick LC, Donaldson K, Clouter A (2001) Impairment of alveolar macrophage phagocytosis by ultrafine particles. Toxicol Appl Pharmacol 172:119–127. doi:10.1006/taap.2001.9128

Sager TM, Porter DW, Robinson VA, Lindsley WG, Schwegler-Berry DE, Castranova V (2007) Improved method to disperse nanoparticles for in vitro and in vivo investigation of toxicity. Nanotoxicology 1:118–129. doi:10.1080/17435390701381596

Saltiel C, Chen Q, Manickavasagam S, Schadler LS, Siegel RW, Menguc MP (2004) Identification of the dispersion

behavior of surface treated nanoscale powders. J Nanopart Res 6:35–46. doi:10.1023/B:NANO.0000023206.45991.dc

Shvedova AA, Kisin ER, Mercer R, Murray AR, Johnson VJ, Potapovich AI et al (2005) Unusual inflammatory and fibrogenic pulmonary responses to single-walled carbon nanotubes in mice. Am J Physiol Lung Cell Mol Physiol 289:L698–L708. doi:10.1152/ajplung.00084.2005

Stumm W, Morgan JJ (1996) Aquatic chemistry. Wiley-Interscience, New York

Teleki A, Wengeler R, Wengeler L, Nirschl H, Pratsinis SE (2008) Distinguishing between aggregates and agglomerates of flame-made TiO2 by high-pressure dispersion. Powder Technol 181:292–300. doi:10.1016/j.powtec.2007.05.016

The Royal Society (2004) Nanoscience and nanotechnologies: opportunities and uncertainties

Tsantilis S, Pratsinis SE (2004) Soft- and hard-agglomerate aerosols made at high temperatures. Langmuir 20:5933–5939. doi:10.1021/la036389w

U.S. EPA (2004) Air quality criteria for particulate matter

Vasylkiv O, Sakka Y (2001) Synthesis and colloidal processing of zirconia nanopowder. J Am Ceram Soc 84:2489–2494

Verwey EJW, Overbeek JTg (1948) Theory of the stability of lyophobic colloids. Elsevier, Amsterdam

von Klot S, Peters A, Aalto P, Bellander T, Berglind N, D'Ippoliti D et al (2005) Ambient air pollution is associated with increased risk of hospital cardiac readmissions of myocardial infarction survivors in five European cities. Circulation 112:3073–3079. doi:10.1161/CIRCULATIONAHA.105.548743

Wallace WE, Keane MJ, Murray DK, Chisholm WP, Maynard AD, Ong TM (2007) Phospholipid lung surfactant and nanoparticle surface toxicity: lessons from diesel soots and silicate dusts. J Nanopart Res 9:23–38. doi:10.1007/s11051-006-9159-5

Warheit DB, Laurence BR, Reed KL, Roach DH, Reynolds GAM, Webb TR (2004) Comparative pulmonary toxicity assessment of single-wall carbon nanotubes in rats. Toxicol Sci 77:117–125. doi:10.1093/toxsci/kfg228

Warheit DB, Webb TR, Reed KL, Frerichs S, Sayes CM (2007) Pulmonary toxicity study in rats with three forms of ultrafine-TiO2 particles: differential responses related to surface properties. Toxicology 230:90–104. doi:10.1016/j.tox.2006.11.002

Wengeler R, Teleki A, Vetter M, Pratsinis SE, Nirschl H (2006) High-pressure liquid dispersion and fragmentation of flame-made silica agglomerates. Langmuir 22:4928–4935. doi:10.1021/la053283n

Widegren J, Bergstrom L (2002) Electrostatic stabilization of ultrafine titania in ethanol. J Am Ceram Soc 85:523–528